2018 IEEE International Conference on Systems, Man, and Cybernetics

Stochastic relationships between the normal and shear interaction forces during tactile exploration of textures

Hikaru Hasegawa, Shogo Okamoto, Hatem Elfekey, and Yoji Yamada
Department of Mechanical Systems Engineering
Nagoya University, Aichi, Japan

***Abstract*—Humans recognize textures through the interaction induced by the normal and shear forces generated between the fingertip and the surface of objects when sliding their fingers on material surfaces. We investigated the stochastic relationships of these two axial forces during tactile exploration. The characteristic values of the elliptical distribution obtained by the variations of the two axial forces were analyzed. It was found that the sizes, shapes, and gradients of the elliptical distribution of the low and high frequency forces statistically varied among the 18 types of textures. These parameters may be the indicators to distinguish the unevenness of the surface and the behavior of friction between the surface and the fingertip. The fact that the stochastic relationships between the two axial forces depend on the surface would help us understand human texture perception.**

***Index Terms*—tactile exploration, normal and shear forces, statistical values**

I. Introduction

Texture sensation depends on the interaction forces induced between the surface of objects and the fingertip or the deformation of the fingertip during tactile exploration. Thus far, researchers have attempted to investigate the relationships between the finger-material interaction and the texture sensation. Many studies reported that the vibration components of a force or deformation of the skin influence the haptic sensation [1]–[6]. These studies discussed the relationships between vibration frequency and haptic sensation for instance, by associating them with the frequency characteristics of the mechanoreceptors. The vibration frequency conveyed to the finger in the normal direction corresponds to the surface profile frequency of the objects and influences the roughness sensation [1], [2]. Besides, the sensation of roughness is affected by the shear force and the friction [3], [4] and the friction models of the interaction between the surface and the fingertip have been investigated (e.g., [7], [8]). Although the haptic sensation is affected by both the normal and shear forces, the relationships between these forces and the haptic sensation have not been investigated in a convergent way.

Previous studies found that stochastic information represented by the power spectrum of force acting on the fingertip or its skin deformation determine the tactile sensations experienced from materials (e.g., [9]–[11]). This idea has been employed by the principles of tactile texture displays that present virtual textures based on the strength of vibratory cues applied to the fingertip in the frequency domain [12]–[14]. These studies indicate inherent linkages between tactile sensations of surfaces and the stochastic behaviors of contact forces in the frequency domain.

The representative characteristic value regarding the two axial forces is the friction coefficient, which is defined as the ratio of normal force to shear force. Most of the previous studies that measured these two axial forces dealt with this macroscopic value (e.g., [15]). However, other statistical values calculated from the two axial forces have not been investigated yet. For instance, a covariance matrix calculated from the time series data of the two axial forces provides substantial information. Although Platkiewicz et al. [16] measured the two axial forces, they did not focus on their stochastic relationships, which have not been investigated thoroughly.

We measured the two axial forces induced by exploring 18 types of textures and calculated the statistical values in several frequency ranges. Then, the characteristic values of the material were extracted by applying a principal component analysis. Few studies have investigated the stochastic relationships between the two axial forces during tactile exploration. We obtained five components that indicate the power of two axial forces, the correlation between the two axial forces, and friction coefficient. Especially, the power of two axial forces in high frequency range implies the power of the friction-induced vibration. Also, the correlation of the two axial forces implies the unevenness of the surface profile. The results of this study would help understand the texture sensation mechanism and could be applied as a new method to detect the texture of surface by touch sensors.

II. Force measurement between fingertip and material and methods

A. Measurement setup

We used the two-axial-force sensing unit shown in Fig. 1 for measuring the normal and shear interaction forces generated between the fingertip and a material sheet during tactile exploration. A similar unit was used in [17]. We employed two single-axial load cells (9313AA2, Kistler, Switzerland), which were located on both sides of an aluminum base for measuring the normal force. Furthermore, a high-precision load cell (9217A, Kistler, Switzerland) was fixed between the two aluminum plates above the normal force sensors for

2577-1655/18/$31.00 ©2018 IEEE
DOI 10.1109/SMC.2018.00515

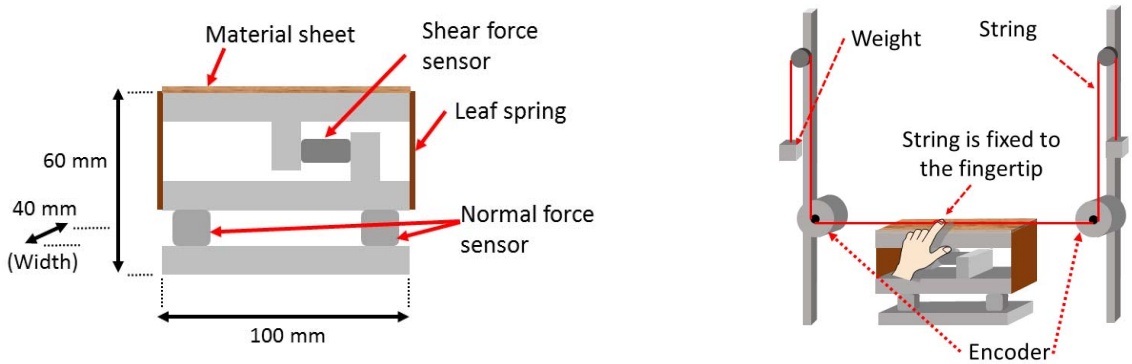

Fig. 1: Left: Schematic view of the force-sensing unit. Right: Measurement setup.

measuring the shear force. Leaf springs fixed to both sides of the upper aluminum plates decoupled the two axial forces. The size of the top surface was 40 $\times$ 100 mm. The signals from both the normal and shear force sensors were amplified by two charge amplifiers (5073A and 5015, Kistler, Switzerland) and transmitted to a computer at the sampling frequency of 2 kHz, which is enough to detect the frequency response of human touch.

The finger motion during tactile exploration was measured by two optical encoders (RE30E, Nidec Copa Electronics Co., Japan). A string that passed through a pulley which was attached to the axis of each encoder was taped on the fingertip. The string was tensioned by small weights, thus the finger position was measured by the encoders through the string. The tension of this string was small enough to ignore its influence on the finger movement.

B. Material

We employed 18 types of textures, as shown in Fig. 2, for measuring the interaction forces. We selected textures that we often touch in our daily life. Cork and coarse Japanese paper induce intensive friction. Thus, we prepared another pair of these textures with talc on their surface for lubrication. Consequently, we measured the interaction forces generated between the fingertip and the surface of 20 samples of textures.

C. Tasks and participants

Participants stroked the material sheet fixed on the upper surface of the force-sensing unit, as shown in Fig. 3, with their dominant index finger. They repeatedly slid their finger on the material surface in one direction for 20 s. They were instructed to slide their finger as if they were investigating the quality of the material. No instructions were provided regarding the speed and force of the finger. Nonetheless, the force data while the finger velocity was in the range between 30 mm/s to 100 mm/s were used for the latter analysis. Five voluntary students (all men, 21–23 years old, all right handed, unaware of the research objectives) participated in the task.

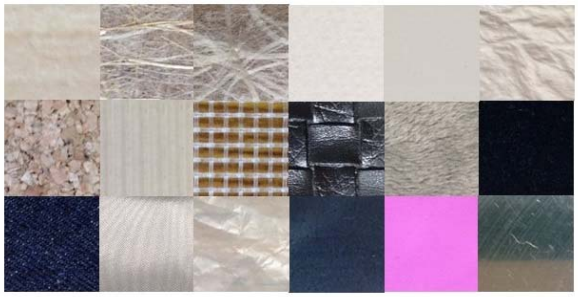

Fig. 2: To measure the force, 18 kinds of material were used. Upper row (from left): wood, coarse Japanese paper, fine Japanese paper, drawing paper, coated paper, and crumpled paper. Middle row: cork, corrugated paper, woven resin wire mesh, fake leather, fake fur, and felt. Bottom row: denim, polyester cloth, polyethylene sheet, rubber, sticky rubber (rubber glove), and flat aluminum

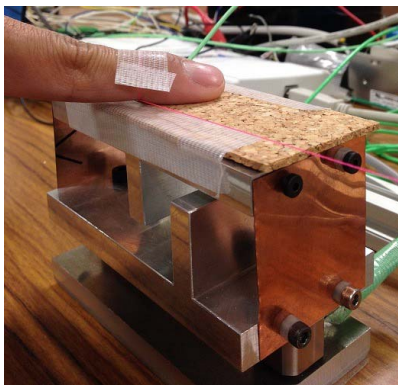

Fig. 3: Photograph of the force measurement setup.

III. Data Analysis

A. Extraction into frequency ranges

The vibration frequency conveyed to the finger during tactile exploration influences the haptic sensation [1]–[3], [5], [6].

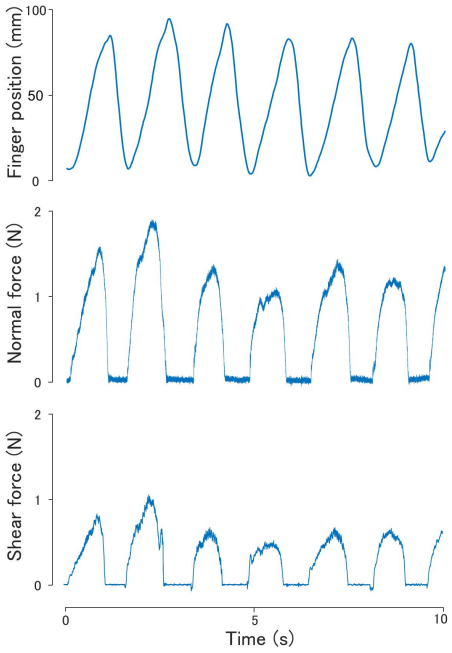

Fig. 4: Finger position and two-axial force data during stroking a woven resin wire mesh.

Therefore, we extracted the force data (e.g., Fig. 4) into five frequency ranges and investigated their characteristics. The spectra in the specific frequency ranges that were obtained by applying the Fourier transform to the two-axial force data were extracted and transformed into force data again by applying the inverse Fourier transform. This process plays a role of a filter to extract the specific spectra. The data with the frequency component in the 0–300 Hz range were extracted in five levels (0–1 Hz, 2–5 Hz, 5–30 Hz, 30–150 Hz, and 150–300 Hz), while the data with frequency over 300 Hz were ignored because of the S/N ratio problem. Although these ranges were determined in an arbitrary manner, in the latter analysis, we found that they were finally divided into two ranges: 0-30 Hz and 30-300 Hz.

B. Statistical values of two-axial force distribution

The two-axial force distribution shaped like an ellipsoid, as shown in Fig. 5. Thus, we calculated the length of the major and minor axes, gradient, and centroid of the estimated elliptical distribution shown in Fig. 6 to investigate the characteristic values of the force data in each frequency range. These values were computed by performing the eigenvalue decomposition of the covariance matrix $\mathbf{\Sigma}$ of the two-axial force data. This calculation can be expressed by

$$\mathbf{\Sigma} = (\boldsymbol{v}_1 \quad \boldsymbol{v}_2) \begin{pmatrix} \lambda_1 & 0 \\ 0 & \lambda_2 \end{pmatrix} (\boldsymbol{v}_1 \quad \boldsymbol{v}_2)^{\mathrm{T}} \tag{1}$$

where λ_1, λ_2 ($\lambda_1 > \lambda_2$) are the eigenvalues of $\mathbf{\Sigma}$ and $\boldsymbol{v}_1$, $\boldsymbol{v}_2$ $\in \mathbb{R}^{2\times 1}$ are the corresponding eigenvectors ($|\boldsymbol{v}_{1,2}|$=1).

The major axis indicates the direction along which the two-axial force data vary the most and its length matches

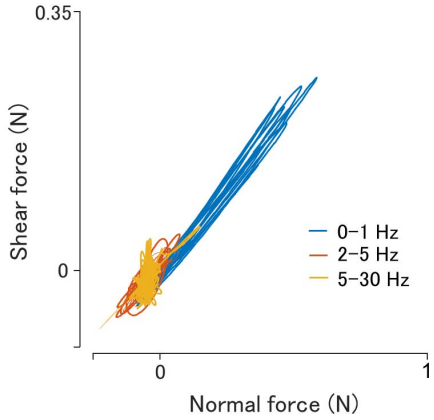

(a) Crumpled paper

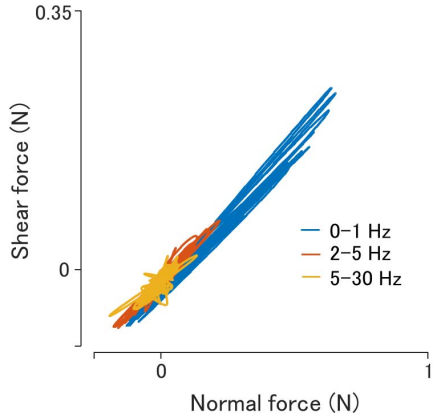

(b) Polyester cloth

Fig. 5: Filtered raw data of the two-axial forces while stroking a (a) crumpled paper and a (b) polyester cloth measured from the same participant. The component greater than 30 Hz are not shown for visual clarity.

the volume of this variance. The major and minor axes are orthogonal and their lengths can be calculated by the square root of each eigenvalue ($\sqrt{\lambda}$). The length of minor axis was larger than the noise level caused during the measurement. The gradient of the ellipsoid was defined as the angle from the normal direction ($\angle \boldsymbol{v}_1$). The two-axial force distributions of 18 types of material shaped inclined ellipsoids and none of them shaped a perfect circle. Thus, the gradient of the ellipsoid can be always determined and indicates the variance ratio of the normal and shear forces. The ratio between the two axial lengths was also calculated as a variable that is not influenced by how strong the touch is performed. This ratio was calculated by dividing the length of the major axis by the length of the minor axis (≥ 1). Thus, this indicates the proportion of force variation toward the directions of the major and minor axes, which means the shape of the force distribution. The shape becomes close to a circle when the ratio is approximately 1 and becomes close to a narrow ellipsoid

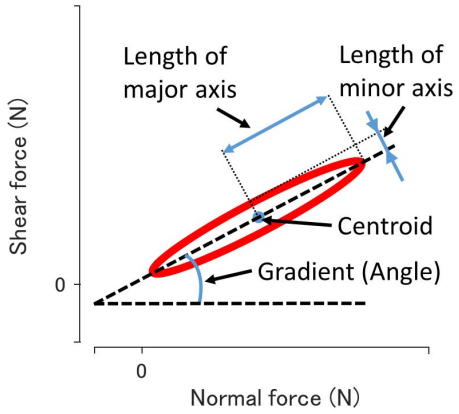

Fig. 6: Statistical values calculated from the elliptical distribution.

when the ratio is large. Although the centroid of the elliptical distribution was calculated as the mean value of the data, we did not discuss about it because of its dependence on the individual finger force.

Based on this, we applied in the latter analysis the two axial lengths, their ratio, and gradient calculated from the two-axial force distribution in each frequency range as the statistical values that indicate the characteristics of the data. These values actually differed among the materials, and thus, the shape of the two-axial force distribution differed between arbitrary two materials, for instance, the crumpled paper and the polyester cloth as shown in Fig. 5. For instance, orange ellipsoids composed by the two-axial forces at 2-5 Hz were distinct between these two types of materials. The ellipsoid measured for a crumpled paper was shorter and more circular and steeper than that of for polyester cloth. Furthermore, the yellow ellipsoids at 5-30 Hz were substantially different between a crumpled paper and polyester cloth.

C. Principal components of the statistical parameters

We investigated the covariance of the the statistical values obtained from the two-axial force data to narrow them. The principal component analysis is the representative method to reveal the covariance of the variables. Thus, we applied this method to four statistical values, which are the two axial lengths, their ratio, and gradient in the five frequency ranges (in total 20 variables). The principal component coefficients of the 20 variables, each of which was transformed into a z-score were calculated. The calculated coefficients were rotated in the promax method for easier interpretation of the components.

The friction induced during tactile exploration differs largely among individuals [18], and thus, we analyzed the data of three participants that exhibited similar trends. We judged the similarity among the data of the participants by the Euclidean distance between the vectors, including 20 statistical values, as shown in Table I. The distances among three participants (A, B, and C) were small, which meant that they exhibited high similarity. Thus, we applied the principal component analysis to the data of these three participants. We also confirmed that the results obtained by analyzing the data of these three participants were similar to that by analyzing the data of all participants.

TABLE I: Euclidean distances among the vectors of statistical values of each participant. Participants A, B, and C exhibited a high similarity.

Participant	A	B	C	D	E
A	–	21.9	21.1	26.0	29.5
B	–	–	24.7	23.8	27.1
C	–	–	–	27.6	29.2
D	–	–	–	–	22.4

IV. Results

By applying the principal component analysis to the data of three participants who exhibited high similarity, five components were extracted. These components explained 80% of the data variation. Table II summarizes the results obtained by rotating the coefficients in the promax method. The oblique rotation angle between each component after rotation in promax method was sufficiently small. This affirms that the orthogonality between the components was still kept even after the rotation. Thus, the five components extracted by the analysis are independent to each other.

From the component coefficient, the first component implied the length of the two axes of the elliptical distribution in the high frequency range (30–300 Hz). These coefficients were of the same sign; thus, the variances of the two axial lengths were linked, e.g., increasing and decreasing together. The second component was the ratio of the two axial lengths of the elliptical distribution in the low frequency range (0–30 Hz). The third and fifth components were the gradients of the elliptical distribution in the high and low frequencies, respectively. The fourth component was the length of the two axes of elliptical distribution in the low frequency range (0–30 Hz). Similar results were obtained by analyzing the data of all participants.

V. Discussion: Explanation of components

The axial length of the elliptical distribution indicates the force variation in the axis direction. This corresponds to the amplitude when the behavior of the two axial forces is considered as a vibration in the time domain. In addition, this corresponds to the power density in the frequency domain, which was extensively investigated in previous studies. The low-frequency component (comp. 4) and the high-frequency component (comp. 1) were extracted independently in this study. Thus, we suggest that the interaction forces during tactile exploration can be discussed separately in the low and high frequencies. This result is supported by the fact that the mechanical receptor unit FAI, which respond to the low-frequency component, and FAII, which respond to the high-frequency component, work selectively by the frequency range [19]. Furthermore, the two-axial force distribution in high

TABLE II: Component coefficients after rotation in the promax method. Relatively small values are gray.

Variables	Frequency [Hz]	Component 1 Power of high freq.	Component 2 Regularity of two axial forces	Component 3 (Friction coeff. at high freq.)	Component 4 Power of low freq.	Component 5 Friction coeff. at low freq.
Major axis (Length)	0–1	-0.10	0.46	0.20	0.17	-0.08
	2–5	-0.09	0.47	0.05	0.37	0.11
	5–30	0.19	0.18	-0.11	0.30	0.00
	30–150	0.46	0.00	0.04	-0.01	0.02
	150–300	0.52	-0.06	0.10	-0.03	-0.06
Minor axis (Length)	0–1	-0.02	0.03	-0.03	0.54	-0.16
	2–5	-0.09	-0.05	-0.01	0.46	0.08
	5–30	0.09	-0.06	0.03	0.40	0.00
	30–150	0.42	-0.08	0.04	0.04	-0.01
	150–300	0.48	-0.05	0.09	-0.05	0.03
Ratio of two axes	0–1	-0.03	0.37	0.09	-0.19	0.00
	2–5	-0.02	0.45	0.06	-0.15	0.02
	5–30	0.07	0.38	-0.24	0.00	0.03
	30–150	0.19	0.21	-0.20	-0.10	-0.04
	150–300	-0.07	0.07	0.11	-0.02	-0.31
Gradient (Angle)	0–1	-0.04	0.05	0.06	-0.12	0.57
	2–5	0.00	0.03	-0.04	0.00	0.52
	5–30	0.00	-0.04	0.11	0.03	0.49
	30–150	0.07	0.11	0.66	-0.08	0.13
	150–300	0.14	0.04	0.62	0.06	-0.08

frequency range of slippery materials (e.g., drawing paper and cork with powder) were relatively small ellipsoid as shown in Fig. 7 (top). On the other hand, those of the relatively sticky materials (e.g., rubber, coated paper and polyethylene sheet) were large ellipsoids. Thus, the size of the two-axial force distribution in high frequency (comp. 1) implies the friction-induced vibration. They are typically greater than 50 Hz [20].

The ratio between the two axial lengths which was extracted as the second component indicates the shape of the distribution. Especially, whether the force distribution is sharp or round depends on whether the relationships between the two axial forces are regular or not. When the shape is sharp, the correlation between the two axial forces is large, and the relationships between the two axial forces are more regular than when the distribution is round, which means that the relationships between the two axial forces are random. Therefore, this component indicates the correlation between the variation of normal and shear forces. We suggest that this correlation explains the unevenness of the surface because the phase difference between the normal and shear force become large when the surface is undulated [8], [21]. In fact, the two-axial force distribution of uneven material (e.g., woven resin wire mesh and corrugated paper) were round and the distribution of relatively even material (e.g., coated paper, cork, and aluminum) were sharp ellipsoid (see Fig. 7 (middle)). Thus, this component may be related to the macroscopic roughness of the material.

The gradients of the elliptical distribution, which were extracted in the third and fifth components, indicated the ratios of variation of the two axial forces, and they correspond to the friction coefficient. Especially, the variation ratio in the two axial forces in the low frequency range corresponds to the kinetic friction coefficient. A larger gradient corresponds to a larger friction coefficient. In fact, the material that induce large friction (e.g., sticky rubber and aluminum) and the material that induce small friction (e.g., coarse Japanese paper, wood, and drawing paper) were distinguished by the score of this component (see Fig. 7 (bottom)). Moreover, the variation ratio in the high frequency range was not discussed in the previous studies. Although the meaning of this component is unclear, it was definitely extracted as an independent factor from other components.

As stated above, we determined not only the variation of the each of the two axial forces but also the shape and gradient of the two-axial force distribution, which have not been discussed in previous studies. We acquired the results by investigating the stochastic relationships between the two axial forces. The relationships between the five components obtained in this study and the haptic sensation of materials should be further investigated.

VI. Conclusion

In the present study, we investigated the stochastic relationships between the normal and shear forces induced between the fingertip and 18 types of material sheets by measuring these forces. We calculated four statistical values in five frequency ranges (0–1 Hz, 2–5 Hz, 5–30 Hz, 30–150 Hz, and 150–300 Hz) obtained by the variation of the force data. These were the lengths of the major and minor axes, their ratio, and gradient of the elliptical distribution from the two-axial force data. A principal component analysis was applied to the data of participants to extract either covariant or independent information among these statistical values. As a result, it was revealed that the sizes and gradients of the two-axial force distributions in both the low- and high-frequency ranges and the shape of the distribution in the low frequency

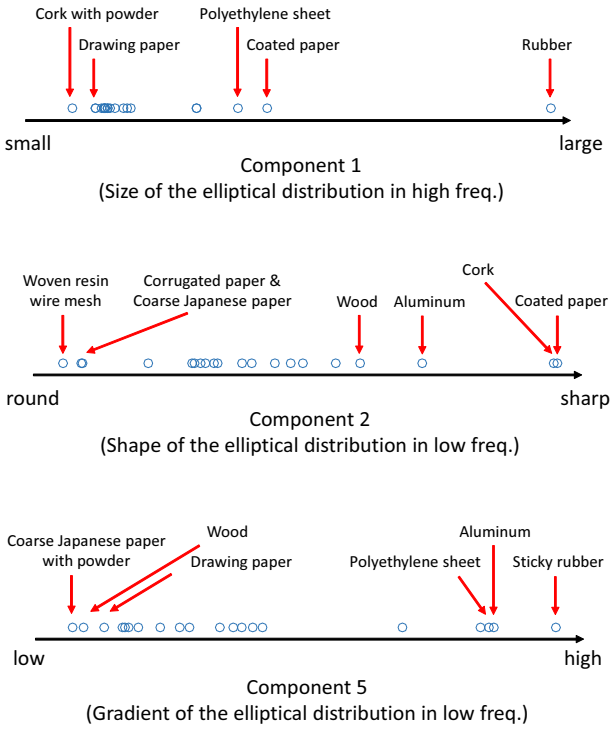

Fig. 7: The distribution of 20 samples of material used in the force measurement on the component axis. Mean component scores among the three participants. The two components are not shown because of their unclarity and page limitation.

range differed among the materials. Especially, the size of the two-axial force distribution in high frequency range implies the power of the friction-induced vibration and the shape of this distribution implies the unevenness of the surface. Also, the gradient of the two-axial force distribution in low frequency range indicates the friction coefficient. Moreover, the gradients of the two axial forces at high frequency and their distribution shapes are new parameters that can be revealed by investigating the stochastic relationship between the two axial forces. The results of this study indicate the importance of focusing on the stochastic relationships between the normal and shear forces induced during tactile exploration to reveal the mechanism of texture sensations.

Acknowledgements

This work was partly supported by MEXT KAKENHI (17H04697).

References

[1] L. Manfredi, H. Saal, K. Brown, M. Zielinski, J. Dammann, V. Polashock, and S. Bensmaïa, "Natural scenes in tactile texture," *Journal of neurophysiology*, vol. 111, 2014.

[2] R. Fagiani, F. Massi, E. Chatelet, Y. Berthier, and A. Akay, "Tactile perception by friction induced vibrations," *Tribology International*, vol. 44, no. 10, pp. 1100 – 1110, 2011.

[3] R. L. Klatzky and S. J. Lederman, "The perceived roughness of resistive virtual textures: I. rendering by a force-feedback mouse," *ACM Trans. Appl. Percept.*, vol. 3, no. 1, pp. 1–14, 2006.

[4] A. M. Smith, C. E. Chapman, M. Deslandes, J.-S. Langlais, and M.-P. Thibodeau, "Role of friction and tangential force variation in the subjective scaling of tactile roughness," *Experimental Brain Research*, vol. 144, no. 2, pp. 211–223, 2002.

[5] S. Okamoto and Y. Yamada, "Lossy data compression of vibrotactile material-like textures," *IEEE Transactions on Haptics*, vol. 6, no. 1, pp. 69–80, 2013.

[6] M. Wiertlewski, J. Lozada, and V. Hayward, "The spatial spectrum of tangential skin displacement can encode tactual texture," *IEEE Transactions on Robotics*, vol. 27, no. 3, pp. 461–472, 2011.

[7] M. Janko, Z. Zhao, M. Kam, and Y. Visell, "A partial contact frictional force model for finger-surface interactions," in *Proc. IEEE Haptic Symposium*, 2018, pp. 255–261.

[8] Y. Fujii, S. Okamoto, and Y. Yamada, "Friction model of fingertip sliding over wavy surface for friction-variable tactile feedback panel," *Advanced Robotics*, vol. 30, no. 20, pp. 1341–1353, 2016.

[9] S. A. Cholewiak, K. Kim, H. Z. Tan, and B. D. Adelstein, "A frequency-domain analysis of haptic gratings," *IEEE Transactions on Haptics*, vol. 3, no. 1, pp. 3–14, 2010.

[10] M. Wiertlewski, C. Hudin, and V. Hayward, "On the 1/f noise and non-integer harmonic decay of the interaction of a finger sliding on flat and sinusoidal surfaces," in *Proceedings of the IEEE World Haptics Conference*, 2011, pp. 25–30.

[11] S. J. Bensmaïa and M. Hollins, "Pacinian representations of fine surface texture," *Perception & Psychophysics*, vol. 67, no. 5, pp. 842–854, 2005.

[12] T. Yamauchi, S. Okamoto, M. Konyo, and S. Tadokoro, "Real-time remote transmission of multiple tactile properties through master-slave robot system," in *IEEE International Conference on Robotics and Automation*, 2010, pp. 1753–1760.

[13] D. Allerkamp, G. Böttcher, F. Wolter, A. C. Brady, J. Qu, and I. R. Summers, "A vibrotactile approach to tactile rendering," *Visual Computing*, vol. 23, pp. 97–108, 2007.

[14] H. Culbertson and K. J. Kuchenbecker, "Importance of matching physical friction, hardness, and texture in creating realistic haptic virtual surfaces," *IEEE Transactions on Haptics*, vol. 10, no. 1, pp. 63–74, 2017.

[15] L. Skedung, K. Danerlöv, U. Olofsson, C. M. Johannesson, M. Aikala, J. Kettle, M. Arvidsson, B. Berglund, and M. W. Rutland, "Tactile perception: Finger friction, surface roughness and perceived coarseness," *Tribology International*, vol. 44, no. 5, pp. 505 – 512, 2011.

[16] J. Platkiewicz, A. Mansutti, M. Bordegoni, and V. Hayward, "Recording device for natural haptic textures felt with the bare fingertip," in *Haptics: Neuroscience, Devices, Modeling, and Applications*, 2014, pp. 521–528.

[17] S. Okamoto, M. Wiertlewski, and V. Hayward, "Anticipatory vibrotactile cueing facilitates grip force adjustment during perturbative loading," *IEEE Transactions on Haptics*, vol. 9, no. 2, pp. 233–242, 2016.

[18] A. Klöcker, M. Wiertlewski, V. Théate, V. Hayward, and J.-L. Thonnard, "Physical factors influencing pleasant touch during tactile exploration," *PLOS ONE*, vol. 8, pp. 1–8, 2013.

[19] S. J. Bolanowski, G. A. Gescheider, R. T. Verrillo, and C. M. Checkosky, "Four channels mediate the mechanical aspects of touch," *The Journal of the Acoustical Society of America*, vol. 84, no. 5, pp. 1680–1694, 1988.

[20] M. Konyo, H. Yamada, S. Okamoto, and S. Tadokoro, "Alternative display of friction represented by tactile stimulation without tangential force," in *Haptics: Perception, Devices and Scenarios*, M. Ferre, Ed., 2008, pp. 619–629.

[21] G. Robles-De-La-Torre and V. Hayward, "Force can overcome object geometry in the perception of shape through active touch," *Nature*, vol. 412, pp. 445–448, 2001.